nature astronomy

Article

https://doi.org/10.1038/s41550-023-02125-3

Quasi-periodic sub-pulse structure as a unifying feature for radio-emitting neutron stars

Received: 20 June 2022

Accepted: 9 October 2023

Published online: 23 November 2023

Check for updates

Michael Kramer [1,2,3] ✉, Kuo Liu [1,3] ✉, Gregory Desvignes[1], Ramesh Karuppusamy [1] & Ben W. Stappers[2]

Magnetars are highly magnetized rotating neutron stars that are predominantly observed as high-energy sources. Six of this class of neutron star are known to also emit radio emission, so magnetars are a favoured model for the origin of at least some of the fast radio bursts (FRBs). If magnetars, or neutron stars in general, are indeed responsible, sharp empirical constraints on the mechanism producing radio emission are required. Here we report on the detection of polarized quasi-periodic substructure in the emission of all well-studied radio-detected magnetars. A correlation previously seen, relating substructure in pulsed emission of radio-emitting neutron stars to their rotational period, is extended and now shown to span more than six orders of magnitude in pulse period. This behaviour is not only seen in magnetars but in members of all classes of radio-emitting rotating neutron stars, regardless of their evolutionary history, their power source or their inferred magnetic field strength. If magnetars are responsible for FRBs, it supports the idea of being able to infer underlying periods from sub-burst timescales in FRBs.

Neutron stars manifest themselves in several classes. Arguably, the most extensively studied one is that of Galactic rotation-powered radio pulsars, with their emission properties investigated across the electromagnetic spectrum[1,2]. 'Normal' pulsars have an average rotation period of about 0.6 s, but some of those range from a few tens of milliseconds after birth to a few seconds or up to 23 s for old pulsars[3], or possibly even 76 s (ref. 4). The 'millisecond pulsars' have periods of a few milliseconds, obtained after a spin-up phase via mass accretion from a binary companion, which 'recycles' a previously 'dead' radio pulsar to enable it to become radio emitting again.

Among the most energetic neutron stars are those of the class called 'magnetars', neutron stars with typical rotation periods of 1–12 s. They emit high-energy outbursts powered by their extremely large (~10^{15} G) magnetic fields[5], which can trigger transient radio emissions as seen in six magnetars so far[5–7].

Recently, interest in magnetars and their properties heightened further by their possible connection to 'fast radio bursts' (FRBs), which are millisecond-long bursts of radio emission from extra-galactic sources[8,9]. The origin of FRBs is not yet understood, but the models discussed can apparently explain certain observed FRB features, such as spectra or characteristic frequency sweeps[10,11]. Some differences in the emission properties have been identified between signals from FRBs that are observed to repeat[12] and those, where no repeating signal has been detected so far[13]. Currently about 24 FRBs, or about 5% of the detected FRBs, are known to have emitted more than one burst[14]. It is not clear whether all non-repeating FRBs will eventually be seen to repeat[15,16].

While the verdict on the existence of (at least two) distinct FRB source populations is still out, the origin of repeating FRB signals is clearly associated with non-cataclysmic processes. Soon after the

[1]Max-Planck-Institut für Radioastronomie, Bonn, Germany. [2]Jodrell Bank Centre for Astrophysics, The University of Manchester, Manchester, UK. [3]These authors contributed equally: Michael Kramer, Kuo Liu. ✉e-mail: mkramer@mpifr-bonn.mpg.de; kliu@mpifr-bonn.mpg.de

discovery of FRBs, magnetars were speculated to be a source of FRBs due to their energetic nature[17]. The recent outburst of the Galactic magnetar, SGR J1935+2154, showed some FRB-like properties[18–20], lending credence to such an association, although questions—for instance, whether magnetar radio emission is luminous enough to explain FRBs—still remain (for example, see ref. 21).

If FRBs are indeed associated with magnetars, one may also expect to detect periodicities in repeating FRBs that are related to the rotation of the underlying neutron star, that is, in the range of a few seconds to tens or possibly hundreds of seconds. However, an attempt to find a periodicity between 1 ms and 1,000 s, for instance, in hundreds of bursts from FRB 20121102A has not been successful[22]. In contrast, on sub-burst timescales, quasi-periodic substructure was reported[23–25] for several bursts from FRBs, though we note that the significance of some detections has been questioned[25]. Such FRB sub-burst structure has been likened to quasi-periodic 'micropulses' seen in radio pulsars (for example, ref. 23).

The short-duration micropulses in radio pulsars have a typical width, τ_μ, and often appear quasi-periodically with a quasi-periodicity, P_μ. They are often superimposed on top of wider sub-pulses comprising the individual pulses for each rotation[1]. It has been long established for normal, non-recycled pulsars that both τ_μ and P_μ scale with the rotational period $P_\mu \approx 10^{-3}P$ and $\tau_\mu \approx 0.5P_\mu$ (refs. 26–28), respectively. Recently, it has also been found that micropulses (also called 'microstructure') can be observed in recycled millisecond pulsars[29,30] at very short periods, which follow the same trend. Hence, while the names 'microstructure' or 'micropulses' were coined after discovering this emission feature in observations of pulsars with slow spin periods (in the approximate range of 0.2–3.0 s) (refs. 27,31), in light of an increasing range of timescales (see below), we suggest it is more appropriate to refer to it as 'quasi-periodic substructure' that is linked to the pulsar rotation period.

In this work, we show that this quasi-periodic substructure is detectable in members of all subclasses of radio-emitting neutron stars, especially in radio-loud magnetars, and that the previously observed dependence of substructure quasi-periodicity on rotational period is still obeyed. This may support attempts[23,25,30] to potentially infer underlying rotational periods from FRBs, if they were indeed emitted by extra-galactic magnetars. More importantly, however, the observation provides a unifying feature that links the radio emission of members in all subclasses of radio-emitting neutron stars.

Data

To perform this study, we collected data from all radio-loud magnetars known so far: XTE J1810−197, Swift J1818.0−1607, PSR J1622−4950, 1E 1547.0−5408 (also known as PSR J1550−5418), PSR J1745−2900 and SGR J1935+2154. In addition, we included the recently discovered source GLEAM-X J162759.5−523504.3, which has also been considered as an ultra-long-period magnetar[32]. Due to the typically flat flux-density spectrum of radio-loud magnetars, our study has been conducted using data obtained at relatively high radio frequencies (that is, typically several gigahertz), except for GLEAM-X J162759.5−523504.3, which was only seen at frequencies below 230 MHz. For XTE J1810−197 and Swift J1818.0−1607, we conducted new polarization observations of individual pulses using the Effelsberg 100-m radio telescope (Methods). for each of the two sources, the observations were made at 6 GHz on three different epochs (Extended Data Table 1). The data were recorded as a filterbank in all four Stokes parameters, with a total bandwidth of 4 GHz and time and frequency resolution of 131 μs and 0.976 MHz, respectively. We removed the frequency dependent time delay caused by free electrons along the line of sight and formed a series of pulses which correspond to each individual rotation of the magnetar (that is, single-pulse data). The single-pulse data were then calibrated for polarization and flux density and cleaned to remove radio interference. For the rest of the sources, the data were collected from either public archives or published literature and analysed accordingly. See Methods for more details.

Results

The best studied radio-detected magnetar is XTE J1810−197 (ref. 6); quasi-periodic substructure in its pulses was suggested during its first phase[33] and more recent phase[34,35] of radio emission. Even though neither work reported a value for the quasi-periodicity, our result appears to be fully consistent with the previous qualitative discussion.

With this work, we have demonstrated the existence of quasi-periodic substructure in all radio-loud magnetars (Fig. 1), except for SGR J1935+2154 for which there are too few detected pulses with sufficient time resolution so far to make a clear detection (Methods); we note, however, that fine-structure was recently reported in sub-pulses on timescales of 5 ms (ref. 36).

The ability to detect quasi-periodic substructure depends crucially on the time resolution and the signal-to-noise ratio, while the strength of the source can vary with time, especially for magnetars (for example, ref. 37). But even under similar observing conditions, quasi-periodic sub-pulses are not ubiquitous and are not always detectable. For instance, the magnetar PSR J1622−4950 shows such structure very prominently in observations in 2017, but less clearly before or later in 2018 (Methods). This is very similar to what is also observed in normal pulsars[38]. Therefore, it is possible that SGR J1935+2154 may reveal quasi-periodic substructure in a later, larger sample of pulses (see, for example, ref. 36).

Examples of the detected quasi-periodic substructure from four of the sources, XTE J1810197, Swift J1818.0−1607, PSR J1622−4950 and GLEAM-X J162759.5−523504.3 are displayed in Fig. 1. We measure the quasi-periodicities (P_μ) and widths (τ_μ) and list them in Extended Data Table 2, which also summarizes values compiled from the literature (Methods). Similar to normal pulsars[38] and millisecond pulsars[30] (Extended Data Table 3), when quasi-periodic substructure is detected (Methods), we measure a range of values forming a source-specific distribution (with one or two clearly preferred values) for the typical quasi-periodicities and widths measured (see, for example, Supplementary Information). Using the geometrical mean as a robust measure, the values of quasi-periodicities measured for magnetars are shown as red symbols in Figs. 2 and 3 and in Extended Data Fig. 1. Strikingly, magnetars show not only quasi-periodic substructure but its quasi-periodicity also follows the same scaling with rotational period that was established for normal pulsars and millisecond pulsars (Fig. 2). This even extends to the recently discovered 76-s PSR J0901−4046, where pulses are also observed to show a set of (otherwise well-defined) quasi-periodicities in single pulses[4]. The source establishes the existence of ultra-long-period neutron stars and also suggests a connection to magnetars[4].

One can even go further by considering the also recently discovered pulsating radio source GLEAM-X J162759.5−523504.3 with a period of 1,090 s, which is also speculated to be an ultra-long-period neutron star or, specifically, an old magnetar[32]. We have analysed the available data and also identified quasi-periodic substructure in its pulses (Methods). But, just as discussed for magnetars and normal pulsars, it is only detectable in a limited range of epochs. The measured quasi-periodicity is somewhat larger than a $P_\mu \approx 10^{-3}P$ scaling would suggest, that is, we measure a value of 6.6 ± 0.6 s. While we discuss this further below, the measurement fits the general trend, extending the observed relationship to about six orders of magnitude. Fitting a power law to the whole range of sources, we obtain $P_\mu = (0.94 \pm 0.04) \times P^{(0.97\pm0.05)}$ ms, where P is in seconds, confirming the previously inferred scaling of $P_\mu = 10^{-3}P$ (refs. 26,27,39) determined for normal pulsars alone.

Interestingly, the recent discovery of a Rotating Radio Transient (RRAT), RRAT J1918−0449, with the Five-Hundred-Meter Aperture Spherical Telescope (FAST), allows us to resolve and, for to our knowledge, the first time, detect quasi-periodic substructure in pulses from

https://doi.org/10.1038/s41550-023-02125-3

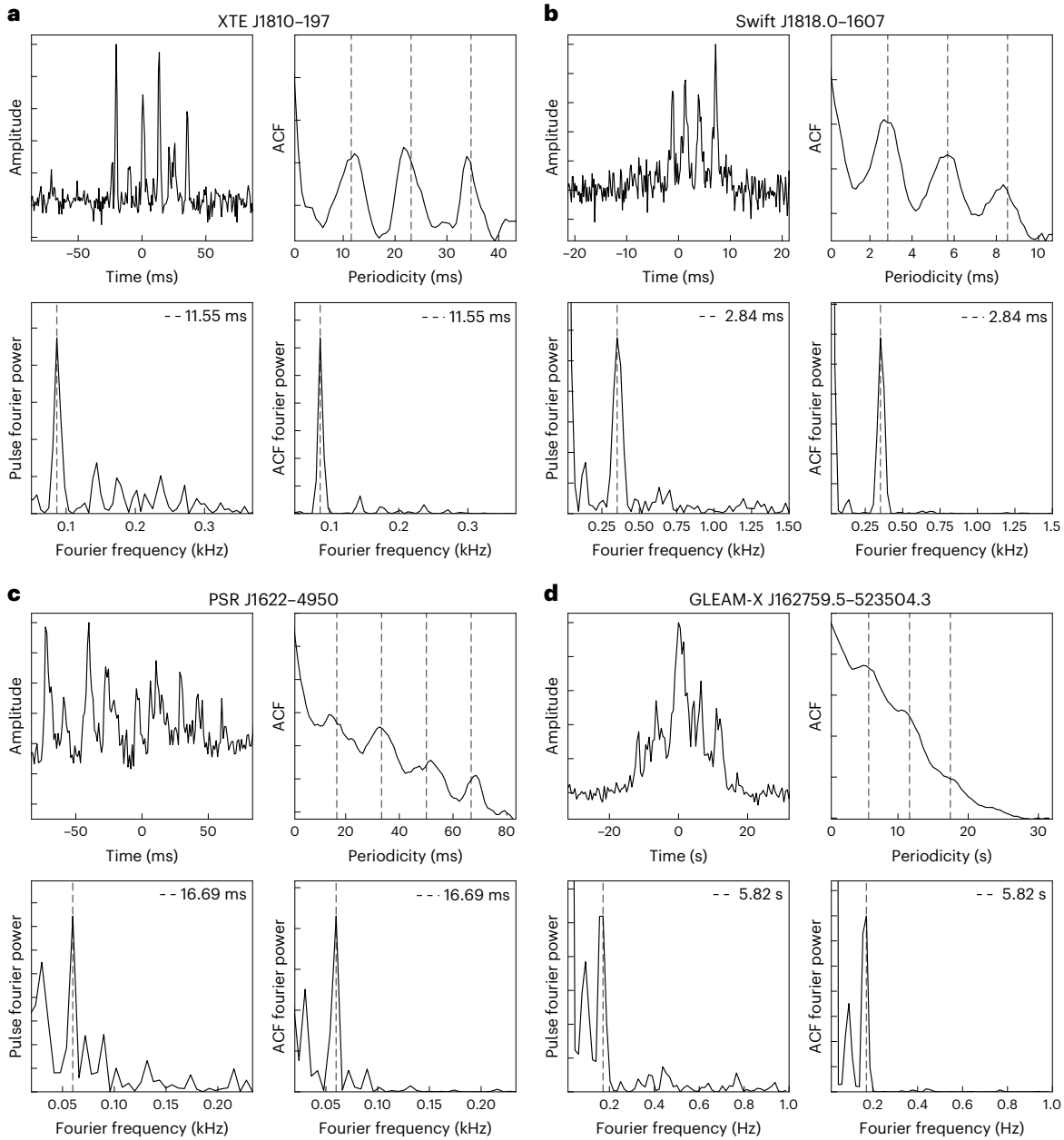

Fig. 1 | Examples of quasi-periodic substructure from four sources. a, For selected source XTE J1810−197, the pulse amplitude as a function of time (upper left graph), the ACF of the pulse (upper right graph), the Fourier PSD of the pulse (lower left graph) and the PSD of the ACF (lower right graph). **b**, For selected source Swift J1818.0−1607, the same. **c**, For selected source PSR J1622−4950, the same. **d**, For selected source GLEAM-X J162759.5−523504.3, the same. In **a**,**b**,**c**,**d**, the vertical dashed lines mark the identified quasi-periodicity and its harmonics in the ACF graphs and their corresponding fundamental frequency in the PSD graphs. Vertical axes are linear arbitrary units.

RRATs[40]. The measured quasi-periodicity agrees perfectly with our scaling law (Fig. 2).

The measurements of the substructure width, τ_μ, are sometimes more difficult to obtain than those of quasi-periodicities, as pointed out for normal pulsars[41]. This results in fewer measurements or larger uncertainties, but we also find a linear scaling with rotational period as shown in Extended Data Fig. 1 and express this fit to the data as $\tau_\mu = (0.59 \pm 0.03) \times P^{(0.99\pm0.02)}$ ms, where P is in seconds. This is consistent with previous findings from normal pulsars alone, but now also expanded in period range and, more particularly, in the type of radio-emitting neutron star.

Given that both independently measured quantities τ_μ and P_μ obviously depend on rotational period P, we also perform a joint fit for those sources, where both measurements can be made. We determine the joint power-law index α and the independent scale factors A_P and A_τ, that is, $P_\mu = A_P \times P^\alpha$ ms and $\tau_\mu = A_\tau \times P^\alpha$ ms, where P is in seconds. We again confirm a linear dependency on rotational period, $\alpha = 1.03 \pm 0.04$, while the spacing of the quasi-periodic sub-pulse structure is approximately twice their width, that is, $A_P = 1.12 \pm 0.14$ and $A_\tau = 0.50 \pm 0.06$. The results are shown in Fig. 3.

Discussion

We have established a universal relationship between the rotational period and emission features that can be found in members of every type of radio-emitting neutron star. The relationship scales simply with the rotational period and applies regardless of the formation or evolutionary history of the neutron star, its presumed energy source, or the regularity (or sporadicity) of its radio emission.

https://doi.org/10.1038/s41550-023-02125-3

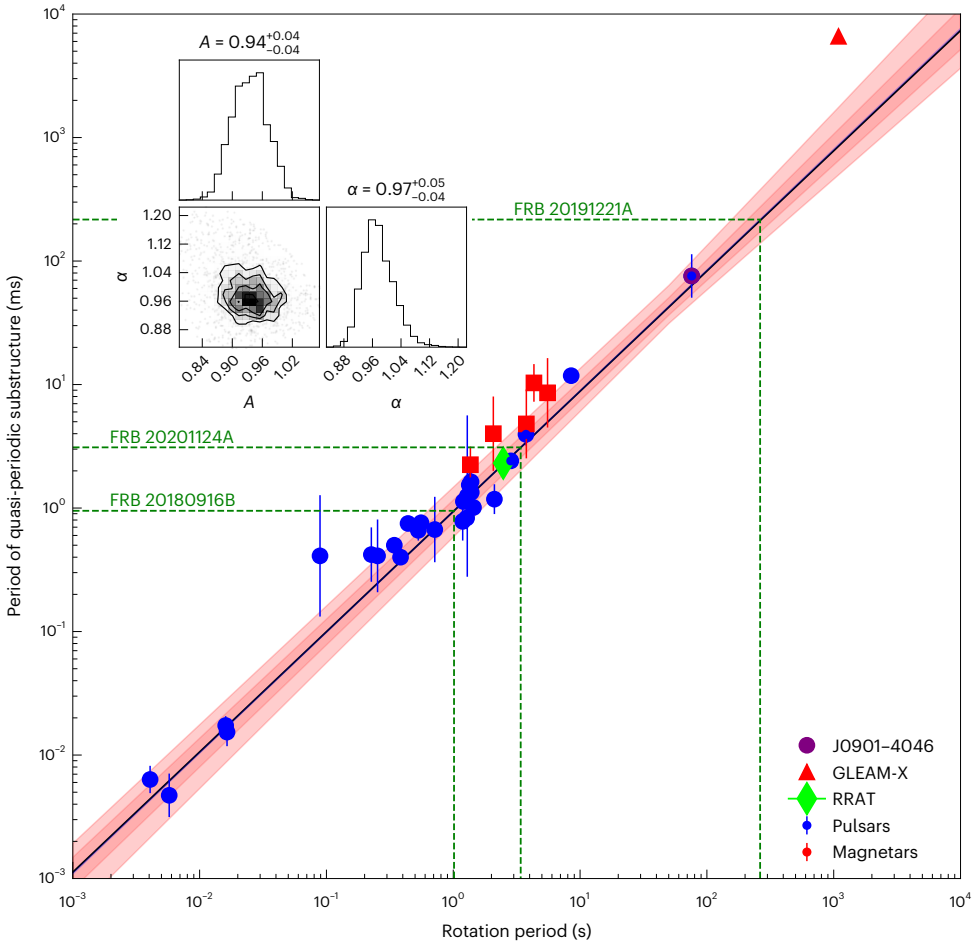

Fig. 2 | Observed relationship of the quasi-periodicity, P_μ, in the observed substructure as a function of neutron star rotation period. Normal pulsars and millisecond pulsars are shown as blue circles; magnetars studied here are shown as red squares; the 76 s pulsar, PSR J0901−4046, is marked as a purple circle; GLEAM-X J162759.5−523504.3 is marked with a red triangle. Each data point represents the geometrical mean with errorbars determined by the geometric standard deviation (Methods). A power law, $P_\mu = A \times P^\alpha$, has been fitted to the data, giving a linear relationship, that is, $P_\mu = (0.94 \pm 0.04) \times P^{(+0.97 \pm 0.05)}$ ms, where P is in seconds. The top-left inset shows a corner plot of the posterior distributions of the joint model parameters, with the off-diagonal elements representing the correlations between parameters and the diagonal elements denoting the marginalized histograms. The ~1σ range of uncertainty in the obtained power law is indicated as a shaded red band. The value of a quasi-periodicity identified for the bursts of a RRAT J1918−0449 is shown as a lime-coloured thin diamond; the RRAT also follows the relationship exactly. Interpreting quasi-periodicities in FRBs as originating from a similar phenomenon, one can use the observed values to infer underlying rotational periods associated with a potential neutron star origin as previously proposed by refs. 23,25,30. To demonstrate this, we select a number of FRB quasi-periodicities that were reported as being significant (>3σ) in refs. 23,24,87.

The relationship extends over about six orders of magnitude, but some deviations are observed. First, the quasi-periodic substructure seen in magnetar pulses is not always present and, second, the periodicities vary to some extent, leading to a classification as a quasi-periodicity within a pulse and leading to a narrow distribution of quasi-periods from pulse-to-pulse that is specific for a given source (this is already well known for many normal pulsars and was also recently established for the 76 s PSR J0901−4046 and shown here for GLEAM-X J162759.5−523504.3). Hence, the similarity goes beyond the existence of the scaling relationship itself. Future measurements will help to establish and constrain the range of values further to identify more commonality.

Clearly, the scatter in the measurements around the predicted values is caused to some extent by the observed fluctuation in periodicities around preferred values. We can speculate whether the measured magnetar periodicity values tend to be somewhat physically larger than those values for normal pulsars, as suggested by Fig. 2, but the deviations by themselves are hardly statistically significant given the uncertainties (Methods). Similar thoughts should also apply to the measurements for GLEAM-X J162759.5−523504.3. But here, we also note that unlike for the other magnetars studied here, the observations of GLEAM-X J162759.5−523504.3 were made at a rather low frequency of $\lesssim$230 MHz.

Even though pulsar substructure properties are usually consistent across large frequency ranges (for example, refs. 27,38), observations at lower frequencies could lead to broader substructures and larger spacing compared to the much higher radio frequencies used here otherwise (see, for example, ref. 28). At the moment, the limited range of epochs prevents further studies.

The origin of the quasi-periodic substructure in the radio emission has been a matter of debate since it was first discovered in normal pulsars. It was interpreted either as a temporal or angular phenomenon[27]. A temporal phenomenon would suggest emission patterns which originate ultimately from processes in the interior or on the surface of neutron stars (for example, ref. 42). In contrast, interpreting the observations as an angular pattern, the quasi-periodic substructure represents 'beamlets' of a characteristic angular width that sweep across the observer with the pulsar rotation[27]. It has already been argued for normal pulsars[28] that a P_μ–P correlation is more naturally explained as an angular pattern. Given the extent of the relationship in period

https://doi.org/10.1038/s41550-023-02125-3

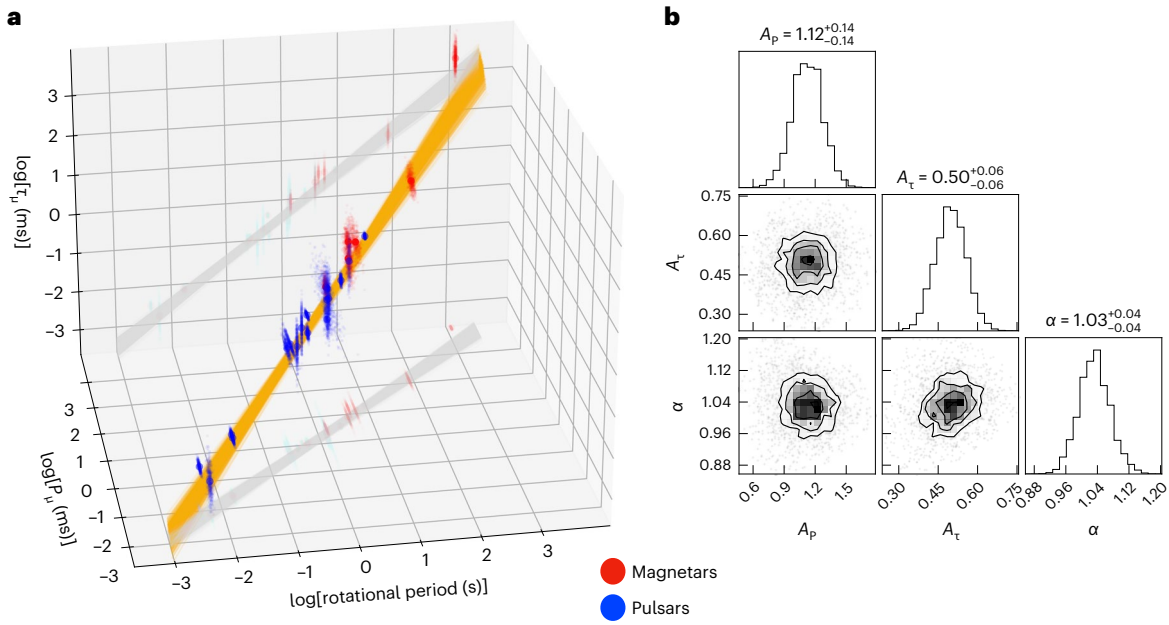

Fig. 3 | Results of a simultaneous fit of substructure periodicity and width to the rotational period. a, Description of the quasi-periodicity $P_\mu = A_P P^\alpha$ ms and width, $\tau_\mu = A_\tau P^\alpha$ ms, where P is in seconds, as a power law with a joint index α. The studied radio-loud magnetars PSR J0901−4046 and GLEAM-X J162759.5−523504.3 are marked in red; the values obtained for pulsars obtained from the literature (Methods) are marked in blue. Each data point represents the geometrical mean surrounded by a cloud with a size determined by the geometric standard deviation (Methods). The shaded ~1σ uncertainty-band of solutions is shown in yellow with projections on the corresponding planes. **b**, A corner plot of the posterior distributions of the joint model parameters, with the off-diagonal elements representing the correlations between parameters and the diagonal elements denoting the marginalized histograms. We find $A_P = 1.12 \pm 0.14$, $A_\tau = 0.50 \pm 0.06$ and $\alpha = 1.03 \pm 0.04$.

space, and to members of all types of radio-emitting neutron stars, an angular beamlet interpretation of the quasi-periodic substructure appears as the only viable explanation. Interestingly, recent work[43,44] appears to derive the exact relationship that we see in Fig. 2. Applying their experience with Tokamak fusion experiments, it connects radio emission of rotating neutron stars to slow tearing instabilities feeding off an inhomogeneous twist profile within the open pulsar circuit[43]. In this picture, radio emission occurs as coherent curvature emission created by Cerenkov-like instabilities of current-carrying Alfven waves in thin current sheets with relativistic particle flow[44]. The model, which also applies to magnetars, predicts that beamed radio emission is created from packets of charged particles, with quasi-periodic substructure being a natural consequence. The encountered timescales are constrained by relativistic beaming, leading to derivation of a scaling relationship where the relevant timescale depends only on the angular frequency Ω and an effective gamma-factor, $\gamma_{\rm eff}$, that is $t_\mu \approx 1/\Omega\gamma_{\rm eff}$, predicting a period dependency of the order of $10^{-3}P$ (ref. 44), as we observe. Even though a range of size structures may be present in the current profile in the pulsar circuit, possibly explaining the fluctuation in the observed quasi-periodicities of a particular source, only the largest are visible due to the smearing effect of relativistic emission[43,44]. The universality of the scaling law shown here suggests that the effective gamma-factor may be the same for all radio-emitting neutron stars, that is, $\gamma_{\rm eff} \approx 200$.

The fundamental dependence of emission substructure (that is quasi-periodicities and also pulse width) (Figs. 2 and 3 and Extended Data Fig. 1) on rotational period among all types of radio-loud rotating neutron stars is especially intriguing for the magnetic-field-powered magnetars, even though young (rotation-powered) pulsars and magnetars have been known to show some similarities in their emission features[2,45]. Radio pulsars usually have a steep flux-density spectrum[1], whereas the spectrum of younger pulsars tends to be flatter[46] and that of magnetars is usually very flat or even inverted[37,47], or may be complex in some cases[48].

By contrast, the polarization features of magnetars and young and energetic pulsars (defined here as those with $\dot{E} > 10^{35}$ erg s^{-1}) are very similar. The latter often show a very large degree of linearly polarized emission[49], while magnetars are also typically 100% linearly polarized[2,45]. The corresponding position angle (PA) of the average pulse profile of pulsars usually shows a distinct variation as a function of pulse duration[49], but it tends to be flatter or irregular for magnetars[2,45]. However, quasi-periodic substructure from individual rotations in normal pulsars can also exhibit an apparently flat PA swing[41]. Our observations (Extended Data Fig. 2) clearly demonstrate that this is also the case for polarized quasi-periodic substructure emission in magnetars.

It has been noted before that these magnetar polarization features are akin to those of bursts from repeating FRBs[50], although exceptions exist[51,52]. If magnetars are indeed responsible for some or all FRBs, suggestions that quasi-periodic substructures in FRBs may be similar to that in normal pulsars[24,30,53] would imply that similar plasma processes (and not vibrations of the neutron star[54]) are responsible. If periodicities abide by the same scaling law, one can follow suggestions in refs. 23,25,30 to use the observed timescales for deriving the underlying rotation period, as also demonstrated in Fig. 2. In this case, one may wonder why underlying rotation periods have not yet been detected, for example in detailed studies of FRB repeaters such as ref. 22. However, the ability to find a periodicity can be hampered severely if the pulse window were to extend over a large fraction of the rotational period[55]. Indeed, magnetar radio emission tends to have much wider duty cycles than normal pulsars[2]. For instance, PSR J1622−4950 emits across almost the full rotation[56]. A large pulse duty cycle may be caused by a non-dipolar magnetic field structure in magnetars and implies a much wider beam than for normal pulsars, covering a much wider area of sky. If that were also the case for FRBs, it would reduce the number of FRBs inferred from population studies accordingly.

In summary, we have demonstrated the existence of quasi-periodic substructure in the radio emission of members of all types of radio-emitting rotating neutron stars, regardless of their evolutionary

history, their power source or their inferred magnetic field strength. Whether magnetars are related to FRBs remains to be seen, but we have shown that quasi-periodic emission structures exist in the individual pulses of radio-loud magnetars, often showing high polarization with flat position angles, that follows the same dependence on rotational periods as found for normal and millisecond pulsars. This universal relationship now spans six orders of magnitude in rotational period. Considering the various types of radio-emitting neutrons stars as whole, we obtain tantalizing insight that all appear to share some similar fundamental processes in their magnetosphere.

Methods

Observations and data collection

The data utilized for this study resulted from new observations, from re-analysed archival data and from published results, covering all six radio-detected magnetars known to date. New observations of two magnetars, XTE J1810−197 (ref. 6) and Swift J1818.0−1607 (ref. 57), were carried out for each on three epochs using the Effelsberg 100-m radio telescope and its CX-band receiver, which covers observing frequencies of 4–8 GHz. Data acquisition was made with a pulsar backend consisting of two units of the second generation of the Reconfigurable Open Architecture Computing Hardware developed with the Field Programmable Gate Array technique by the CASPER team (https://casper.astro.berkeley.edu/). The data were recorded in 8 bit samples stored in PSRFITS search-mode format[58], with a time resolution of 131 µs and 4,096 frequency channels. Single-pulse data with specifications detailed in Extended Data Table 1 were extracted from the search-mode data stream; this used the PSRFITS_UTILS software toolkit (see https://github.com/demorest/psrfits_utils) and an ephemeris obtained from our regular timing programme on these two sources. Dispersion measures (DMs) of 178.0 and 703.0 cm^{-3} pc were used to de-disperse the data of XTE J1810−197 and Swift J1818.0−1607, respectively[57,59]. Next, the single-pulse data were calibrated for polarization and flux density and cleaned for radio interference using the PSRCHIVE software package[58]. Polarization calibration was obtained using information from an injected noise diode signal associated with the pulsar observation. The data were flux-density calibrated using an exposure on the calibration source NGC 7027 and its catalogued flux-density spectrum[60]. Finally, rotation measures of 74.44 and 1,442 rad m^{-2} were applied to the data of XTE J1810−197 (ref. 6) and Swift J1818.0−1607 (refs. 57,59), respectively, to correct for interstellar Faraday rotation in the linear polarization component.

Data for the magnetar PSR J1622−4950 measured at 3.1 GHz with the Parkes telescope[56] were obtained from the public Australia Telescope National Facility data archive (see https://atoa.atnf.csiro.au); the selection of data focused on epochs when the magnetar was exceedingly bright, allowing for detailed single-pulse analyses. These data are available in PSRFITS search format with total intensity information and specifications detailed in Extended Data Table 1. They were processed to generate single-pulse data with the DSPSR software package, an ephemeris obtained from ref. 61 and a DM of 820 cm^{-3} pc.

Pulsation data on the magnetar-like periodic radio transient GLEAM-X J162759.5−523504.3 were obtained from the data archive published by ref. 32. The observations were carried out with the Murchison Widefield Array at 88 to 215 MHz. In addition, we obtained information on pulse properties of magnetar 1E 1547.0−5408 from data retrieved from the Australia Telescope National Facility archive and collected information from the literature on the well-studied Galactic Centre magnetar, PSR J1745−2900 and the sparsely detected SGR J1935+2154 (see the next section for details).

Measurement of magnetar substructure widths and quasi-periodicities

XTE J1810−197, Swift J1818.0−1607, PSR J1622−4950 and GLEAM-X J162759.5−523504.3: For these three magnetars and the GLEAM source, the substructure quasi-periodicities and widths were measured using auto-correlation analysis. The methodology of this analysis is well summarized in Section 7.4.2.2 of ref. 1 and many other publications (for example, refs. 26,62). Here, the first principle of this methodology is also shown in the sketch in the Supplementary Information. For a given waveform $I(n)$, its auto-correlation function (ACF) is defined as:

$$A(k) = \sum_n I(n+k)I(n). \quad (1)$$

When there is quasi-periodic structure in the pulse, it manifests itself by exhibiting a sequence of equally spaced local maxima in the ACF. The time lag of the first local maximum corresponds to the characteristic separation, that is, quasi-periodicity of the substructure, while those of the rest equal to incremental numbers times the periodicity (Supplementary Information). Thus, the value of the characteristic quasi-periodicity can be defined by the first local maximum in the ACF. To search for quasi-periodic substructure and to determine a value for the periodicity, we first calculated the ACFs for all the single pulses in our data. Then we used a Fourier transform to calculate the power spectral density (PSD) of each pulse, in turn calculated its ACF and in both identified a set of maxima, each of which may correspond to the presence of a periodicity. Next, we cross-checked the two groups of maxima and kept those which were reported in both (within 20% difference in values) as candidates for the periodicity. Finally, we visually checked the pulse profile and its ACF and noted the pulse as a detection only when at least one of the reported periodicities corresponded to a real periodic feature in both the profile and its ACF. The shortest reported candidate periodicity was recorded as the value of the detected quasi-periodicity in the pulse. We investigated 4,798 pulses: 452 from XTE J1810−197; 4,126 from Swift J1818.0−1607; 208 from PSR J1622−4950; and 12 from GLEAM-X J162759.5−523504.3. From these four sources, we detected, respectively, 77, 400, 93 and 2 pulses displaying quasi-periodic substructure. The results are displayed in corresponding figures in the Supplementary Information. We note that for XTE J1810−197, we observed a bimodal distribution of periodicities, as is occasionally observed for normal pulsars[41]. We note that our derived value is at the lower end implied by the averaged ACF shown by ref. 35, whereas a value reported by ref. 34 is consistent with the first peak of our distribution.

We also measured the width of the substructure using the ACF analysis. As in our data, the inverse of the channel bandwidth is smaller than the used sampling times, the width can be defined as the first turning point in the ACF from zero lag (Supplementary Information). Its value corresponds approximately to the Full Width at Half Maximum of the substructure[38,63]. To obtain the turning point for each pulse, a spline fit was conducted on the ACF, starting from the first non-zero lag bin until the first bin before the identified quasi-periodicity, which reported a group of detected knots. Then all reported knots were visually inspected together with the ACF, to identify the exact one that corresponds to the first turning point in the ACF for each pulse.

As observed for normal pulsars, not all individual pulses exhibit identifiable quasi-periodic substructure. Also, as for normal pulsars, a limited range of periodicities can sometimes be observed. This is caused by a mixture of intrinsic variation, the occurrence of harmonically related quasi-periodicities or instrumental and observational constraints (see, for example, refs. 38,62). For this reason, we studied the distribution of values measured for the ensemble of studied pulses. To account for cases where the histogram does not show a single, clearly identifiable peak, we refer to the geometric mean as a robust method to determine a preferred value. In Extended Data Table 2 we quote uncertainties of the geometric mean, x_{geo}, expressed in the form of the geometric standard deviation (GSTD) factor, Δx_{GSTD}, defining a range from $x_{geo}/\Delta x_{GSTD}$ to $x_{geo} \times \Delta x_{GSTD}$. We also quote the mean, the error of the mean and the median for comparison.

There are three more magnetars that have been detected at radio frequencies: 1E 1547.0−5408 (also known as PSR J1550−5418)[64], the Galactic Centre magnetar PSR J1745−2900 (ref. 7) and SGR J1935+2154 (refs. 18–20). Below, we discuss the obtained substructure properties for these sources, using partly archival data and previously published results.

1E 1547.0−5408: This 2.1 s magnetar showed strong transient radio emission, especially after its 2009 outburst[65]. Retrospectively, for this outburst, two strong radio pulses were reported recently[66], which saturated the 1 bit digitization of the observing system and potentially distorted the pulse signal. Thus, studied a different observation with the Parkes telescope from 25 February 2009 (MJD 54887), at 8.3 GHz. With a time resolution of 1 ms, this 30 min observation reveals very narrow pulses leading the main pulse by about 500 ms. To our knowledge, these features have not yet been reported. The recorded subintegrations contain nine periods each, but the spacing of these pulses suggests they are the result of single bright bursts occurring at slightly different rotational phases during the folded 18 s. The pulses are consistent with having a width of $\lesssim$1 ms. Inspecting the spacing of these pulses, one can infer a periodicity of about 4 ms. These estimates are consistent with an analysis of further search-mode data accessible from the archive and recorded during 2016 and 2017, although the available time resolution in that record is also limited to 1 ms. Given these constraints, we consider these measurements with caution but list them for completeness with a GSTD of 2.0.

J1745−2900: This magnetar exhibits the longest duration of uninterrupted detectable radio emission since its first detection in the radio spectrum in 2013 (ref. 7). The profile has been observed to be highly variable in frequency[67] and on short and long timescales[68], with its strength diminishing in recent years[69]. The strong background emission from nearby Sgr A* combined with the relatively long period of 3.76 s causes significant red noise in single-dish time-series measurements with a very large dispersion measure of 1,778 pc cm^{-3}, this implies that high-frequency observations with interferometers are best suited to study the existence of quasi-periodic substructure. Summarizing the wealth of observations, the broad pulse envelope often reveals partly overlapping sub-pulses with clearly discernable short pulses (see, for example, Fig. 3 of ref. 70 or Fig. 4 of ref. 68). The typical intrinsic width of individual emission components is found to be as short as 1.6 ms (ref. 68) or 1.8 ms (ref. 70). Such narrow components, when resolvable, are separated from each other, often in a quasi-periodic fashion, with typical separations from 2.2 ± 0.7 ms (see Figs. 4 and 8 of ref. 68) to about 10.4 ± 1.7 ms (see Fig. 3 of ref. 70). More often, these emission features are somewhat wider and blend into each other, overlapping at about a substructure width. The most common pulse width for all components is 3.2 or 6.4 ms (ref. 68). This is consistent with a recent pulse width measure of 4.9 ± 0.5 ms between 4.4 and 7.8 GHz and corrected for interstellar scattering[69]. For our purposes, we account for the variety of measurements by computing the geometrical mean from the above values, that is, a pulse width of 3.1 ms (with a GSTD of 1.7, cf. Fig. 5 of ref. 68) and a quasi-periodicity of 4.8 ms (GSTD 1.9).

SGR J1935+2154: Efforts to detect radio emission from this 3.24 s magnetar following its outbursts had failed repeatedly, providing stringent upper limits on the existence of detectable radio emission[71]. In contrast, on 28 April 2020, both the CHIME[19] and STARE2 (ref. 18) telescopes detected the same short radio burst from a direction consistent with that of SGR J1935+2154, which were followed by a sequence of detections within a short time window (for example, refs. 72–74). Both CHIME and STARE2 measured a DM around 333 pc cm^{-3}. The CHIME data observed between 400 and 800 MHz revealed two sub-bursts with widths determined to 0.585(14) ms and 0.335(7) ms, respectively, where numbers in parentheses indicate measurement errors, after correcting for apparent effects of multipath scattering (with a thin-screen scattering timescale of 0.759(8) ms when referenced to 600 MHz). Both components were separated by 28.91(2) ms. The STARE2 data taken at higher frequencies between 1,280 MHz and 1,530 MHz showed no significant evidence for scattering[18]. Nevertheless, because CHIME adopted a scattering model, they also fitted a corresponding model, deriving an apparent intrinsic width of 0.61(9) ms and a scattering timescale of 0.4(1) ms when referenced to 1 GHz. Scaling the CHIME scattering time to the same frequency, using the expected radio frequency dependency of ν^{-4} (ref. 9), one finds 0.098(1) ms, which is clearly inconsistent with the STARE2 measurement. Further detections of radio pulses to clarify this matter turned out to be difficult. Observations of the magnetar with the FAST on 30 April 2020, detected a weak radio pulse with a DM consistent with the CHIME and STARE2 events. While this indicated that all three radio pulses were emitted by the magnetar, a reliable width measurement was not reported[75]. Further radio observations had mixed success, mostly reporting non-detections (see, for example, refs. 76,77 and references therein), including even deep unsuccessful FAST observations[78]. A later successful detection with FAST appeared again to be too weak to study the pulse properties[79]. More recently, however, using over 500 h of follow-up observations, two further radio bursts from the magnetar were reported[20]. These bursts showed an observed width of 0.866(43) ms and 0.961(48) ms, respectively, separated in time by about 1.4 s, at a frequency of 1,324 MHz. Attempts to fit a scattering tail to the slightly asymmetric burst shapes derived scattering timescales of 0.315(12) ms and 0.299(29) ms, respectively. At a reference frequency of 1 GHz, this would amount to an average of about 0.952(21) ms, for the expected frequency scaling. Since the three measured timescales are barely consistent with each other, unless one postulates an unusually flat frequency dependence, we follow the discussion in ref. 20. and their suggestion that it is more straightforward to reconcile the measurements by assuming that the slight asymmetries observed in the bursts are actually intrinsic. As the $1/e$ timescale of pulse smearing due to scattering can be usually accounted for, to first order, by adding the widths in quadrature, we derive from the published value estimates for the originally observed pulse width as follows: 0.73(36) ms for the STARE2 detection, 0.96(48) ms and 0.93(41) ms for the two CHIME sub-bursts, respectively. Computing the geometric mean of all five measurements, we derive 0.88 ms and with a GSTD of 1.2. The paucity of events registered for SGR J1935+2154 prevents a study of periodicities within the magnetar bursts, beyond noting that the two CHIME components were separated by 28.91(2) ms. We note, however, that very recently fine-structure was reported in sub-pulses on timescales of 5 ms (ref. 36).

Measurement of pulsar substructure widths and quasi-periodicities

The period scaling of pulse substructure timescales and periodicities was already established for normal pulsars in the late 1970s. Since then, many more measurements have been made, and we attempt to compile them here. Meanwhile, quasi-periodic substructure has been also detected in a sample of millisecond pulsars, which we also include to expand the study of the period scaling to the shortest periods. In recent years, a number of pulsars have been discovered with periods above 10 s and even more recently with even larger periods, as discussed above.

Normal pulsars. Quasi-periodic substructure known as 'microstructure' has been studied extensively for normal pulsars, measuring both width and quasi-periodicities. We compiled a list of values for normal pulsars from refs. 26,27,38,39,62,63 and references therein. We also used quasi-periodicity measurements presented in ref. 41, reevaluated some of their measurements for weak pulsars, based on the data provided by the authors with the publication. Where values differed across different studies, we again computed the geometrical mean and GSTD factors as shown in Fig. 2.

Fast-spinning millisecond pulsars. In recent years, measurements of quasi-periodic substructure have also become available for fast-rotating millisecond pulsars using high-sensitivity and high-time-resolution observations[29,30]. As for normal pulsars, we do not consider measurements of giant pulses (and their nanoshots) as they may have a different origin compared to regular pulsar radio emission[1], but concentrate on the studies of normal pulses emitted by millisecond pulsars. The combined measurements for both the width and quasi-periodicity follow the period scaling, as indicated by refs. 27,29,30,39.

Long-period radio pulsars. Since magnetars share the same period range as long-period pulsars, we also include unusually slowly rotating pulsars, namely the 8.5 s PSR J2144−3933, the 12.1 s PSR J2251−3711 and the 23.5 s PSR J0250+5854. Recently, the presence of quasi-periodic substructure was reported for PSR J2144−3933 (ref. 80) with an estimate of substructure quasi-periodicity (as a median derived from a distribution of 355 single pulses) of $P_\mu = 11.8 \pm 0.6$ ms. The width of the substructure shown in ref. 80 is consistent with a value half this size, hence we estimate $\tau_\mu = 5.9 \pm 0.3$. Accordingly, we convert this into corresponding estimates for the geometric means.

For J2251−3711, ref. 81 presents single pulses with sub-pulses with a typical width of 4 to 16 ms. No clear quasi-periodic substructure is visible, but we tentatively adopt a typical substructure width of 10 ± 6 ms, or in terms of a geometric mean of 9.8 ms with a GSTD of 1.6.

PSR J0250+5854's average profile and single pulses show differences across frequencies[82]. Single pulses have only been detected confidently at 320 MHz, where the strong individual pulses appear only in the first pulse component. However, no reliable detection of quasi-periodic substructure can be made from the published data, preventing us from including it in our analysis.

Rotating radio transients. RRATs are sourced by subset of rotating neutron stars that emit radio pulses sporadically[83]. First considered to be a different class of neutron stars, continued or more sensitive observations allowed association of the emission with an underlying period which increases with time, confirming a rotational origin of the period[84]. Ref. 85 argued that RRATs are not a distinct or a separate population, but an extreme class of ordinary pulsars, which are discovered more easily via their single pulses. Observations of RRATs with sufficient time resolution and sensitivity to reveal potential quasi-periodic substructure are rare. Recently, however, the 2.48-s RRAT J1918−0449 was discovered and monitored with the FAST, showing clear quasi-periodic substructure with a periodicity of $P_\mu = 2.31 \pm 0.25$ ms. The substructure width is measured to be $\tau_\mu = 1.47 \pm 0.25$ ms (ref. 40).

The results of our magnetar measurements, combined with the values for normal pulsars, millisecond pulsars and the recent discoveries of PSR J0901−4046, GLEAM-X J162759.5−523504.3 and RRAT J1918−0449 are shown in Extended Data Tables 2 and 3. They are summarized in Figs. 2 and 3 and Extended Data Fig. 1, for the substructures' quasi-periodicities and widths, respectively.

We have modelled the data with power-law fits. We first conducted a normal least-square fit by minimizing a standard χ^2 expression. This provided initial guesses for two fitted parameters, the power-law index and the scale factor and for their uncertainties. To check for covariances and the shape of posterior distributions, we then employed the UltraNest sampler[86] to perform an analysis with uniform priors, covering a range of ±100 times the uncertainties around the least-squares results. As a likelihood function, we used the usual $\ln(\mathcal{L}) = -\chi^2/2$. The resulting power-law fits and the posterior distributions are presented in the main text and the figure captions. They all have in common that both quantities depend linearly on the rotational period of the neutron star.

With the quasi-periodicities of magnetars somewhat larger than the values implied by the scaling law, we performed a weighted least-squares fit to the magnetar data points alone. We assumed the same linear scaling with rotational period, P, as in Fig. 3 to determine only the scaling factors. We derive for the periodicity: $A_P^M = 1.69 \pm 0.17$ (the superscript M signifying 'for magnetars') which compares to $A_P = 1.12 \pm 0.14$ for the whole dataset. This is a factor of 1.51 ± 0.24 larger. A similar fit for the magnetar substructure widths finds $A_\tau^M = 0.37 \pm 0.10$, which compares to $A_\tau = 0.50 \pm 0.06$, that is being a factor 0.74 ± 0.22 smaller. Both scalings are consistent within 2σ.

Polarization of quasi-periodic substructure

We analysed the polarization of all quasi-periodic substructure from XTE J1810−197 and Swift J1818.0−1607 obtained during our new observations with the Effelsberg 100-m radio telescope. The polarization profile and its corresponding linear polarization PAs of the pulses shown in Fig. 1 and additional examples (shown in the Supplementary Information) are presented in Extended Data Fig. 2. For XTE J1810−197, most substructures are close to be 100% linearly polarized, consistent with a very high degree of linear polarization of the integrated profile of this magnetar. The PA swings of these quasi-periodic substructures are apparently flat within several percent points of the rotational period. For quasi-periodic substructures from Swift J1818.0−1607, the fraction of linear polarization is high on average while exhibiting some distinct pulse-to-pulse variability. In some pulses the linear component can be close to 100% while in others it may not be significant. The PA swings of most substructures are shown to be flat, some with low-level variation on a scale of roughly 10°. These features of the PA swings are similar to what have been seen in quasi-periodic substructures from ordinary pulsars[41].

Data availability

Most data used in this study are available from the literature or already downloaded from publicly accessible archives (see https://atoa.atnf.csiro.au). Magnetar data obtained for this study in particular are available by contacting the corresponding author to arrange the data transfer; these observations generated large volumes of data.

References

1. Lorimer, D. R. & Kramer, M. *Handbook of Pulsar Astronomy* Vol. 4 (Cambridge Univ. Press, 2004).
2. Philippov, A. & Kramer, M. Pulsar magnetospheres and their radiation. *Annu. Rev. Astron. Astrophys.* **60**, 495–558 (2022).
3. Tan, C. M. et al. LOFAR discovery of a 23.5 s radio pulsar. *Astrophys. J.* **866**, 54 (2018).
4. Caleb, M. et al. Discovery of a radio-emitting neutron star with an ultra-long spin period of 76 s. *Nat. Astron.* **6**, 828–836 (2022).
5. Kaspi, V. M. & Beloborodov, A. M. Magnetars. *Annu. Rev. Astron. Astrophys.* **55**, 261–301 (2017).
6. Camilo, F. et al. Transient pulsed radio emission from a magnetar. *Nature* **442**, 892–895 (2006).
7. Eatough, R. P. et al. A strong magnetic field around the supermassive black hole at the centre of the Galaxy. *Nature* **501**, 391–394 (2013).
8. Lorimer, D. R., Bailes, M., McLaughlin, M. A., Narkevic, D. J. & Crawford, F. A bright millisecond radio burst of extragalactic origin. *Science* **318**, 777–780 (2007).
9. Thornton, D. et al. A population of fast radio bursts at cosmological distances. *Science* **341**, 53–56 (2013).
10. Metzger, B. D., Margalit, B. & Sironi, L. Fast radio bursts as synchrotron maser emission from decelerating relativistic blast waves. *Mon. Not. R. Astron. Soc.* **485**, 4091–4106 (2019).
11. Lyubarsky, Y. Emission mechanisms of fast radio bursts. *Universe* **7**, 56 (2021).
12. Spitler, L. G. et al. Fast radio burst discovered in the Arecibo pulsar ALFA survey. *Astrophys. J.* **790**, 101 (2014).
13. Pleunis, Z. et al. Fast radio burst morphology in the first CHIME/FRB catalog. *Astrophys. J.* **923**, 1 (2021).

14. Spanakis-Misirlis, A. FRBSTATS: a web-based platform for visualization of fast radio burst properties. Astrophysics Source Code Library, record ascl:2106.028 (2021).
15. Caleb, M., Stappers, B. W., Rajwade, K. & Flynn, C. Are all fast radio bursts repeating sources? *Mon. Not. R. Astron. Soc.* **484**, 5500–5508 (2019).
16. James, C. W. et al. Which bright fast radio bursts repeat? *Mon. Not. R. Astron. Soc.* **495**, 2416–2427 (2020).
17. Platts, E. et al. A living theory catalogue for fast radio bursts. *Phys. Rep.* **821**, 1–27 (2019).
18. Bochenek, C. D. et al. A fast radio burst associated with a Galactic magnetar. *Nature* **587**, 59–62 (2020).
19. CHIME/FRB Collaborationet al. A bright millisecond-duration radio burst from a Galactic magnetar. *Nature* **587**, 54–58 (2020).
20. Kirsten, F. et al. Detection of two bright radio bursts from magnetar SGR 1935+2154. *Nat. Astron.* **5**, 414–422 (2021).
21. Beloborodov, A. M. Can a strong radio burst escape the magnetosphere of a magnetar? *Astrophys. J.* **922**, L7 (2021).
22. Li, D. et al. A bimodal burst energy distribution of a repeating fast radio burst source. *Nature* **598**, 267–271 (2021).
23. Majid, W. A. et al. A bright fast radio burst from FRB 20200120E with sub-100 nanosecond structure. *Astrophys. J.* **919**, L6 (2021).
24. Chime/FRB Collaboration & Andersen, B. C. et al. Sub-second periodicity in a fast radio burst. *Nature* **607**, 256–259 (2022).
25. Pastor-Marazuela, I. et al. A fast radio burst with sub-millisecond quasi-periodic structure. *Astron. Astrophys.* **678**, A149 (2023).
26. Taylor, J. H., Manchester, R. N. & Huguenin, G. R. Observations of pulsar radio emission. I. Total intensity measurements of individual pulses. *Astrophys. J.* **195**, 513 (1975).
27. Cordes, J. M. Pulsar microstructure: periodicities, polarization and probes of pulsar magnetospheres. *Aust. J. Phys.* **32**, 9–24 (1979).
28. Kramer, M., Johnston, S. & van Straten, W. High-resolution single-pulse studies of the Vela pulsar. *Mon. Not. R. Astron. Soc.* **334**, 523–532 (2002).
29. De, K., Gupta, Y. & Sharma, P. Detection of polarized quasi-periodic microstructure emission in millisecond pulsars. *Astrophys. J.* **833**, L10 (2016).
30. Liu, K. et al. Detection of quasi-periodic micro-structure in three millisecond pulsars with the Large European Array for Pulsars. *Mon. Not. R. Astron. Soc.* **513**, 4037–4044 (2022).
31. Hankins, T. H. Microsecond intensity variation in the radio emission from CP 0950. *Astrophys. J.* **169**, 487–494 (1971).
32. Hurley-Walker, N. et al. A radio transient with unusually slow periodic emission. *Nature* **601**, 526–530 (2022).
33. Serylak, M. et al. Simultaneous multifrequency single-pulse properties of AXP XTE J1810–197. *Mon. Not. R. Astron. Soc.* **394**, 295–308 (2009).
34. Maan, Y., Joshi, B. C., Surnis, M. P., Bagchi, M. & Manoharan, P. K. Distinct properties of the radio burst mission from the Magnetar XTE J1810–197. *Astrophys. J.* **882**, L9 (2019).
35. Caleb, M. et al. Radio and X-ray observations of giant pulses from XTE J1810–197. *Mon. Not. R. Astron. Soc.* **510**, 1996–2010 (2022).
36. Zhu, W. et al. A radio pulsar phase from SGR J1935+2154 provides clues to the magnetar FRB mechanism. *Sci. Adv.* **9**, eadf6198 (2023).
37. Lazaridis, K. et al. Radio spectrum of the AXP J1810–197 and of its profile components. *Mon. Not. R. Astron. Soc.* **390**, 839–846 (2008).
38. Lange, C., Kramer, M., Wielebinski, R. & Jessner, A. Radio pulsar microstructure at 1.41 and 4.85 GHz. *Astron. Astrophys.* **332**, 111 (1998).
39. Keith, M. J. et al. The High Time Resolution Universe Pulsar Survey - I. System configuration and initial discoveries. *Mon. Not. R. Astron. Soc.* **409**, 619–627 (2010).
40. Chen, J. L. et al. The discovery of a rotating radio transient J1918−0449 with intriguing emission properties with the five-hundred-meter Aperture Spherical Radio Telescope. *Astrophys. J.* **934**, 24 (2022).
41. Mitra, D., Arjunwadkar, M. & Rankin, J. M. Polarized quasiperiodic structures in pulsar radio emission reflect temporal modulations of non-stationary plasma flow. *Astrophys. J.* **806**, 236 (2015).
42. Clemens, J. C. & Rosen, R. Observations of nonradial pulsations in radio pulsars. *Astrophys. J.* **609**, 340–353 (2004).
43. Thompson, C. Radio emission of pulsars. I. Slow tearing of a quantizing magnetic field. *Astrophys. J.* **933**, 231 (2022).
44. Thompson, C. Radio Emission of Pulsars. II. Coherence catalyzed by cerenkov-unstable shear alfvén waves. *Astrophys. J.* **933**, (2022).
45. Kramer, M., Stappers, B. W., Jessner, A., Lyne, A. G. & Jordan, C. A. Polarized radio emission from a magnetar. *Mon. Not. R. Astron. Soc.* **377**, 107–119 (2007).
46. Jankowski, F. et al. Spectral properties of 441 radio pulsars. *Mon. Not. R. Astron. Soc.* **473**, 4436–4458 (2018).
47. Torne, P. et al. Submillimeter pulsations from the magnetar XTE J1810−197. *Astrophys. J.* **925**, L17 (2022).
48. Lower, M. E., Shannon, R. M., Johnston, S. & Bailes, M. Spectropolarimetric properties of Swift J1818.0−1607: a 1.4 s radio magnetar. *Astrophys. J.* **896**, L37 (2020).
49. Weltevrede, P. & Johnston, S. Profile and polarization characteristics of energetic pulsars. *Mon. Not. R. Astron. Soc.* **391**, 1210–1226 (2008).
50. Hilmarsson, G. H., Spitler, L. G., Main, R. A. & Li, D. Z. Polarization properties of FRB 20201124A from detections with the Effelsberg 100-m radio telescope. *Mon. Not. R. Astron. Soc.* **508**, 5354–5361 (2021).
51. Luo, R. et al. Diverse polarization angle swings from a repeating fast radio burst source. *Nature* **586**, 693–696 (2020).
52. Kumar, P. et al. Circularly polarized radio emission from the repeating fast radio burst source FRB 20201124A. *Mon. Not. R. Astron. Soc.* **512**, 3400–3413 (2022).
53. Petroff, E., Hessels, J. W. T. & Lorimer, D. R. Fast radio bursts. *Astron. Astrophys. Rev.* **27**, 4 (2019).
54. McDermott, P. N., Van Horn, H. M. & Hansen, C. J. Nonradial oscillations of neutron stars. *Astrophys. J.* **325**, 725–748 (1988).
55. Lazarus, P. et al. Arecibo Pulsar Survey using ALFA. IV. Mock spectrometer data analysis, survey sensitivity, and the discovery of 40 pulsars. *Astrophys. J.* **812**, 81 (2015).
56. Levin, L. et al. A Radio-loud magnetar in X-ray Quiescence. *Astrophys. J.* **721**, L33–L37 (2010).
57. Champion, D. et al. High-cadence observations and variable spin behaviour of magnetar Swift J1818.0−1607 after its outburst. *Mon. Not. R. Astron. Soc.* **498**, 6044–6056 (2020).
58. Hotan, A. W., van Straten, W. & Manchester, R. N. psrchive and psrfits: an open approach to radio pulsar data storage and analysis. *Publ. Astron. Soc. Aust.* **21**, 302–309 (2004).
59. Camilo, F. et al. Radio disappearance of the magnetar XTE J1810-197 and continued X-ray timing. *Astrophys. J.* **820**, 110 (2016).
60. Zijlstra, A. A., van Hoof, P. A. M. & Perley, R. A. The evolution of NGC 7027 at radio frequencies: a new determination of the distance and core mass. *Astrophys. J.* **681**, 1296–1309 (2008).
61. Scholz, P. et al. Spin-down evolution and radio disappearance of the magnetar PSR J1622−4950. *Astrophys. J.* **841**, 126 (2017).
62. Cordes, J. M. Pulsar radiation as polarized shot noise. *Astrophys. J.* **210**, 780–791 (1976).
63. Cordes, J. M., Weisberg, J. M. & Hankins, T. H. Quasiperiodic microstructure in radio pulsar emissions. *Astron. J.* **100**, 1882–1891 (1990).
64. Camilo, F., Ransom, S. M., Halpern, J. P. & Reynolds, J. 1E 1547.0-5408: a radio-emitting magnetar with a rotation period of 2 seconds. *Astrophys. J.* **666**, L93–L96 (2007).

65. Camilo, F., Halpern, J. P. & Ransom, S. M. Radio pulsations not detected from AXP/SGR 1E1547.0–5408 following recent outburst. *Astron. Telegr.* **1907**, 1 (2009).
66. Israel, G. L. et al. X-ray and radio bursts from the magnetar 1E 1547.0–5408. *Astrophys. J.* **907**, 7 (2021).
67. Torne, P. et al. Simultaneous multifrequency radio observations of the Galactic Centre magnetar SGR J1745–2900. *Mon. Not. R. Astron. Soc.* **451**, L50–L54 (2015).
68. Wharton, R. S. et al. VLA observations of single pulses from the Galactic Center magnetar. *Astrophys. J.* **875**, 143 (2019).
69. Suresh, A. et al. 4–8 GHz spectrotemporal emission from the Galactic Center magnetar PSR J1745–2900. *Astrophys. J.* **921**, 101 (2021).
70. Pearlman, A. B., Majid, W. A., Prince, T. A., Kocz, J. & Horiuchi, S. Pulse morphology of the galactic center magnetar PSR j1745–2900. *Astrophys. J.* **866**, 160 (2018).
71. Younes, G. et al. X-ray and radio observations of the magnetar SGR J1935+2154 during Its 2014, 2015, and 2016 outbursts. *Astrophys. J.* **847**, 85 (2017).
72. Bochenek, C. D. et al. Upper limit to radio bursts from SGR 1935+2154 (ATEL 14074) by STARE2. *Astron. Telegr.* **14077**, 1 (2020).
73. Pleunis, Z., CHIME/FRB Collaboration. Properties of the CHIME/FRB 2020 October 8 detections of SGR 1935+2154. *Astron. Telegr.* **14080**, 1 (2020).
74. Dong, F. A., Chime/FRB Collaboration. CHIME/FRB detection of a bright radio burst from SGR 1935+2154. *Astron. Telegr.* **15681**, 1 (2022).
75. Zhang, C. F. et al. A highly polarised radio burst detected from SGR 1935+2154 by FAST. *Astron. Telegr.* **13699**, 1 (2020).
76. Bailes, M. et al. Multifrequency observations of SGR J1935+2154. *Mon. Not. R. Astron. Soc.* **503**, 5367–5384 (2021).
77. Younes, G. et al. X-ray burst and persistent emission properties of the magnetar SGR 1830−0645 in outburst. *Astrophys. J.* **924**, 136 (2022).
78. Lin, L. et al. No pulsed radio emission during a bursting phase of a Galactic magnetar. *Nature* **587**, 63–65 (2020).
79. Zhu, W. et al. FAST detection of radio bursts and pulsed emission from SGR J1935+2154. *Astron. Telegr.* **14084**, 1 (2020).
80. Mitra, D., Basu, R., Melikidze, G. I. & Arjunwadkar, M. A single spark model for PSR J2144−3933. *Mon. Not. R. Astron. Soc.* **492**, 2468–2480 (2020).
81. Morello, V. et al. The SUrvey for Pulsars and Extragalactic Radio Bursts - IV. Discovery and polarimetry of a 12.1-s radio pulsar. *Mon. Not. R. Astron. Soc.* **493**, 1165–1177 (2020).
82. Agar, C. H. et al. A broad-band radio study of PSR J0250+5854: the slowest spinning radio pulsar known. *Mon. Not. R. Astron. Soc.* **508**, 1102–1114 (2021).
83. McLaughlin, M. A. et al. Transient radio bursts from rotating neutron stars. *Nature* **439**, 817–820 (2006).
84. McLaughlin, M. A. et al. Timing observations of rotating radio transients. *Mon. Not. R. Astron. Soc.* **400**, 1431–1438 (2009).
85. Keane, E. F., Kramer, M., Lyne, A. G., Stappers, B. W. & McLaughlin, M. A. Rotating radio transients: new discoveries, timing solutions and musings. *Mon. Not. R. Astron. Soc.* **415**, 3065–3080 (2011).
86. Buchner, J. UltraNest - a robust, general purpose Bayesian inference engine. *J. Open Source Softw.* **6**, 3001 (2021).
87. Niu, J.-R. et al. FAST observations of an extremely active episode of FRB 20201124A. IV. Spin period search. *Res. Astron. Astrophys.* **22**, 124004 (2022).
88. Kardashev, N. S. et al. Pulsar observations with a time resolution of 10 microsec at 102.5 MHz. *Sov. Astron.* **22**, 583–587 (1978).
89. Cordes, J. M. Coherent radio emission from pulsars. *Space Sci. Rev.* **24**, 567–600 (1979).
90. Hankins, T. H. & Boriakoff, V. Microstructure in the pulsar 0950+08 interpulse at radio wavelengths. *Astrophys. J.* **249**, 238–240 (1981).
91. Popov, M. V. et al. Pulsar microstructure and its quasi-periodicities with the S2 VLBI system at a resolution of 62.5 nanoseconds. *Astron. Astrophys.* **396**, 171–187 (2002).
92. Ferguson, D. C. & Seiradakis, J. H. A detailed, high time resolution study of high frequency radio emission from PSR 1133+16. *Astron. Astrophys.* **64**, 27–42 (1978).
93. Boriakoff, V. On the radio pulse emission mechanism of PSR 1133+16: simultaneous dual-frequency high time resolution observations. *Astrophys. J.* **272**, 687 (1983).

Acknowledgements

This manuscript makes use of observations conducted with the 100-m radio telescope in Effelsberg owned and operated by the Max-Planck-Institut für Radioastronomy. We are grateful to D. Lorimer and D. Champion for comments on the manuscript and thank L. Spitler and her group for stimulating discussions. We thank R. Main for useful discussions on microstructure in the FRBs. M.K., K.L. and G.D. acknowledge the financial support by the European Research Council for the ERC Synergy Grant BlackHoleCam under contract no. 610058. B.W.S. acknowledges the financial support by the European Research Council for the ERC Advanced Grant MeerTRAP under contract no. 694745.

Author contributions

M.K. and K.L. drafted the manuscript with suggestions from co-authors. M.K. and K.L. reduced and analysed the Effelberg 100-m radio telescope data and archival data. K.L., G.D. and R.K. conducted observations with the 100-m radio telescope and preprocessed data.

Funding

Open access funding provided by Max Planck Society.

Competing interests

The authors declare no competing interests.

Additional information

Extended data is available for this paper at https://doi.org/10.1038/s41550-023-02125-3.

Supplementary information The online version contains supplementary material available at https://doi.org/10.1038/s41550-023-02125-3.

Correspondence and requests for materials should be addressed to Michael Kramer or Kuo Liu.

Peer review information *Nature Astronomy* thanks the anonymous reviewers for their contribution to the peer review of this work.

https://doi.org/10.1038/s41550-023-02125-3

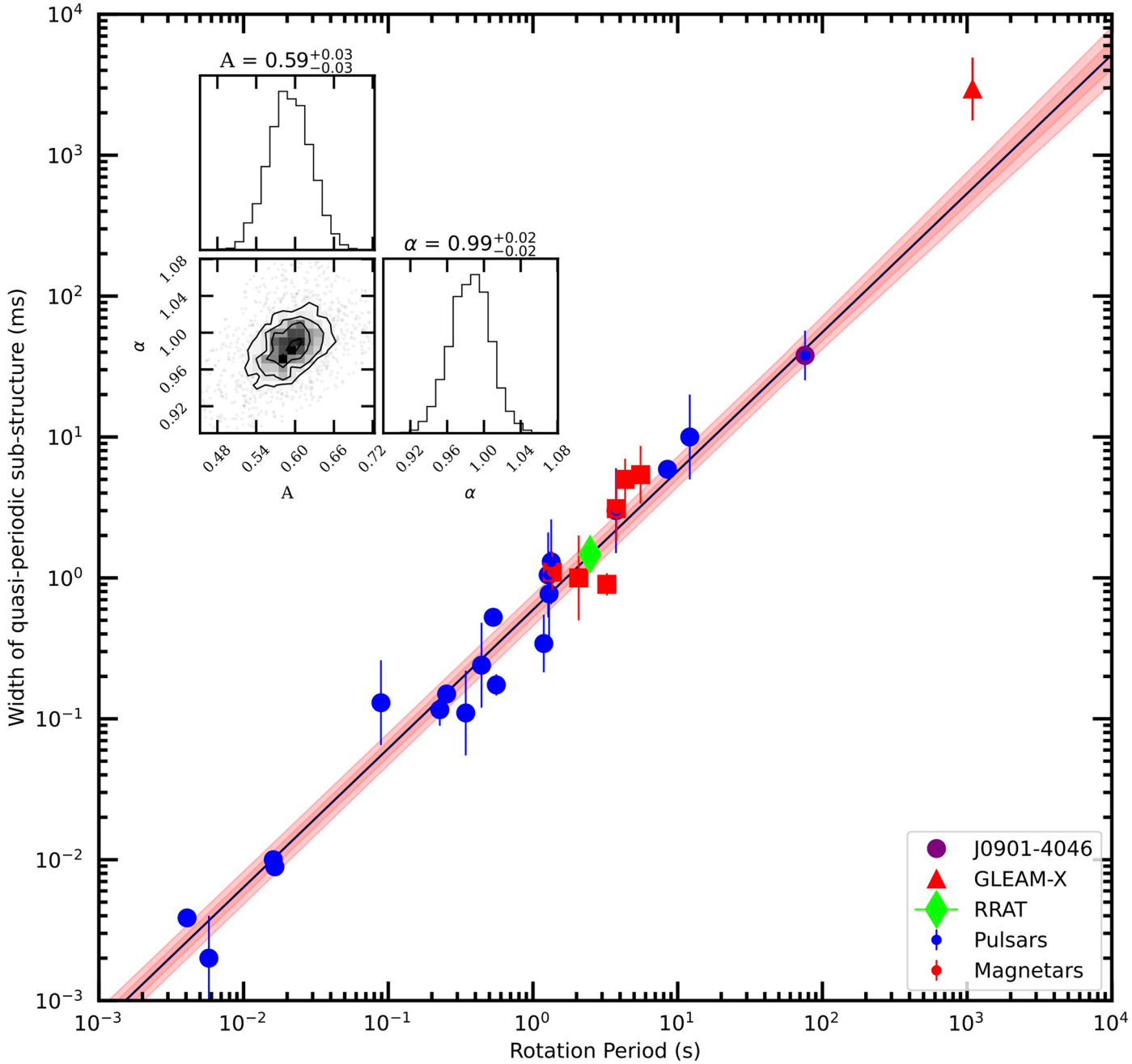

Extended Data Fig. 1 | Observed relationship of sub-structure width, τ_μ, as a function of neutron star rotation period. Normal pulsars and millisecond pulsars are shown as blue circles. Magnetars studied here are shown as red squares. The 76-s PSR J0901 − 4046 considered to be possibly an old magnetar is marked as a red-blue circle. GLEAM-X J162759.5 − 523504.3 is marked with a red triangle. The values obtained for pulsars obtained from the literature (see Methods) are marked in blue. Each data point represents the geometrical mean surrounded by a cloud with a size determined by the geometric standard deviation (see Methods). A power-law, $\tau_\mu = A \times P^\alpha$, has been fitted to the shown data, giving a linear relationship, that is $\tau_\mu = (0.59 \pm 0.03) \times P^{(+0.99 \pm 0.02)}$ ms. The top-left inset shows a corner plot of the posterior distributions of the model parameters, with the off-diagonal elements representing the correlations between the parameters, and the diagonal elements denoting the marginalized histograms. The ~ 1σ range of uncertainty in the obtained power-law is indicated as a shaded red band. A similar linear dependency on rotation period is found for the quasi-periodicities. We also show the width of quasi-periodic sub-structure identified for the bursts of a Rotating Radio Transient RRAT J1918 − 0449 as a lime-coloured thin diamond, which also fits in the relationship exactly.

https://doi.org/10.1038/s41550-023-02125-3

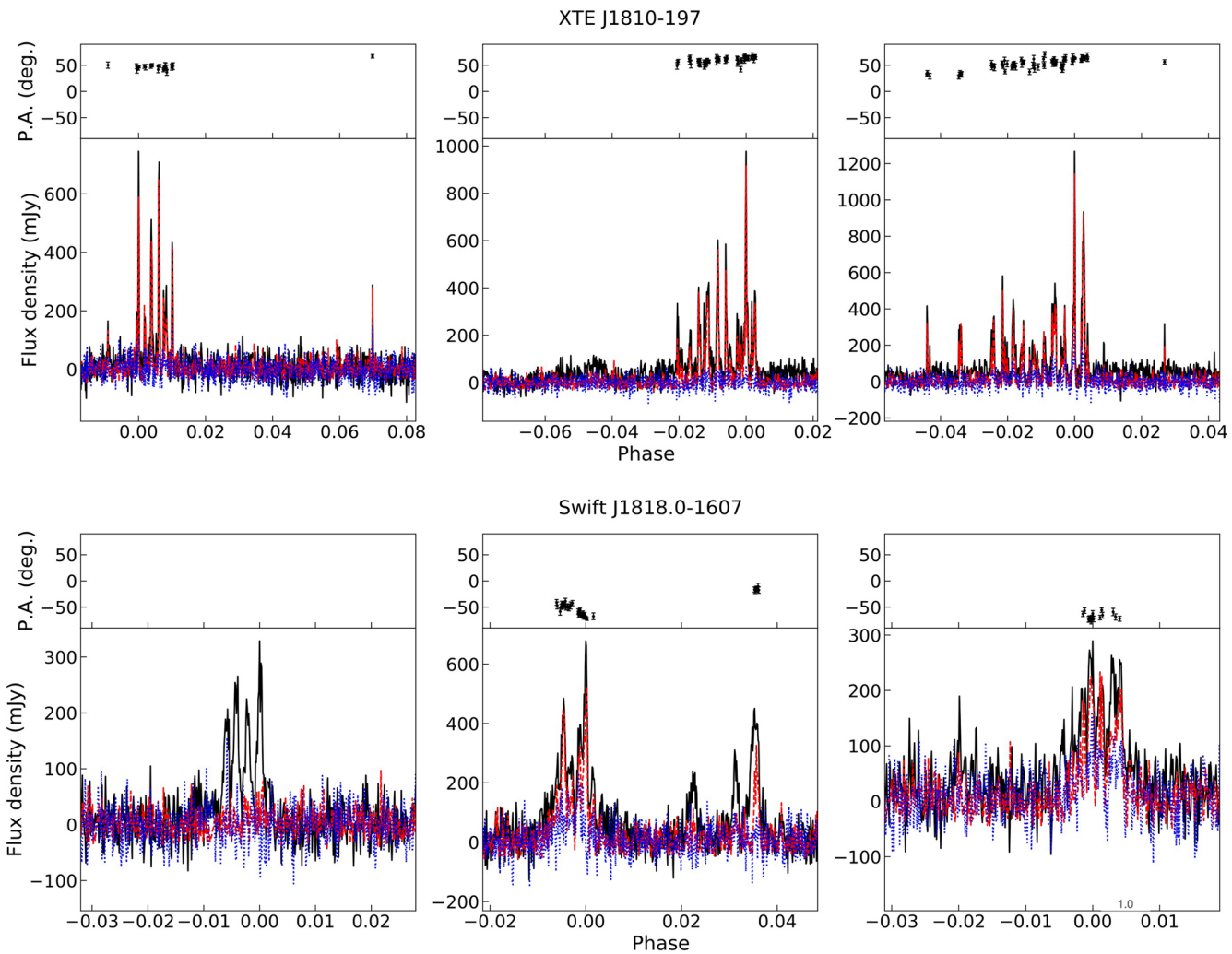

Extended Data Fig. 2 | Polarization profile and polarization angle of the pulses from XTE J1810 − 197 and Swift J1818.0 − 1607. These are the pulses shown in Fig. 1 and the Supplementary Information; XTE J1810 − 197 (**a**) and Swift J1818.0 − 1607 (**b**). The black solid, red dashed and blue dotted lines represent total intensity, linear and circular polarization, respectively. The pulse from Swift J1818.0 − 1607 in the bottom left panel has no significant linear polarization.

https://doi.org/10.1038/s41550-023-02125-3

Extended Data Table 1 | Details of the data analysed for this work

Source	Date	f (GHz)	Δf (MHz)	$t_{\rm obs}$ (min)	δt (ms)
1E 1547.0−5408	2009-02-25	8.3	512	30	1.0
PSR J1622−4950	2017-07-04	3.1	1024	15	1.0
XTE J1810−197	2020-08-10	6.0	4000	15	0.68
	2020-08-28	6.0	4000	14	0.68
	2020-09-25	6.0	4000	13	0.68
Swift J1818.0−1607	2021-02-12	6.0	4000	39	0.17
	2021-07-05	6.0	4000	25	0.17
	2021-09-16	6.0	4000	30	0.17
GLEAM−X J162759.5−523504.3	2018-01-09	0.152	159	-	500

The columns provide the source name, the date of the observation, the central observing frequency (f), bandwidth (Δf), integration time (t_{obs}) and time resolution (Δt) of the data recorded. Data on XTE J1810−197 and Swift J1818.0−1607 were collected with the Effelsberg Radio Telescope, and those on 1E 1547.0−5408 and PSR J1622−4950 were recorded at the Parkes Radio Telescope. Note that the observation of GLEAM−X J162759.5−523504.3 were conducted with the Murchison Widefield Array using its drift scan observing mode, so the integration time is not specified.

https://doi.org/10.1038/s41550-023-02125-3

Extended Data Table 2 | Measured properties of the quasi-periodic sub-structure. For the studied magnetars and GLEAM−X J162759.5−523504.3 (abbreviated below as GLEAM−X) we present the width, τ_μ, and quasi-periodicity, P_μ

Source	P	—— τ_μ ——				—— P_μ ——			
	(s)	MN (ms)	MD (ms)	GM (ms)	GSTD	MN (ms)	MD (ms)	GM (ms)	GSTD
1E 1547.0−5408	2.07	–	–	1.0	2.0	–	–	4.0	2.0
J1622−4950	4.33	5.3 ± 0.1	4.7	5.0	1.4	11.0 ± 0.2	10.0	10.3	1.4
J1745−2900	3.77	–	–	(3.1)	(1.7)	–	–	(4.8)	(1.9)
XTE J1810−197	5.54	6.0 ± 0.4	6.8	5.4	1.6	10.3 ± 0.6	12.0	8.6	1.9
Swift J1818.0−1607	1.37	1.16 ± 0.02	1.0	1.1	1.4	2.37 ± 0.04	2.24	2.2	1.4
SGR J1935+2154	3.24	(0.89 ± 0.04)	(0.93)	(0.88)	(1.2)	–	–	–	–
GLEAM−X	1090.8	3400 ± 1800	3200	3000	1.7	6110 ± 290	6110	6103	1.0

For both quantities, we quote the mean (MN), the median (MD), the geometric mean (GM) and the geometric standard deviation factor (GSTD). For PSR J1745−2900 and SGR J1935+2154 the values are displayed in brackets to indicate that these were derived from the literature, see text for details.

https://doi.org/10.1038/s41550-023-02125-3

Extended Data Table 3 | Published values of sub-structure properties in radio pulsars as compiled from the literature

Source J2000	P (s)	τ_μ GM (ms)	τ_μ GSTD	P_μ GM (ms)	P_μ GSTD	References
0304+1932	1.3876	–	–	1.34	1.2	[41]
0332+5434	0.7145	–	–	0.67	1.8	[38, 87]
0437−4715	0.0058	0.002	2.0	0.005	1.5	[29]
0528+2200	3.7455	3.05	2.0	3.95	1.2	[41, 88]
0546+2441	2.8439	–	–	2.41	1.1	[41]
0659+1414	0.3849	–	–	0.40	1.1	[41]
0814+7429	1.2922	0.77	2.0	1.25	4.5	[65]
0826+2637	0.5307	0.53	1.1	0.66	1.2	[38, 41, 88]
0835−4510	0.0893	0.13	2.0	0.41	3.1	[28]
0837+0610	1.2738	1.05	2.0	0.83	1.2	[41]
0901−4046	75.886	37.9	1.5	75.7	1.5	[4]
0953+0755	0.253 1	0.15	1.1	0.41	2.0	[38, 41, 65, 89, 90]
1022+1001	0.0165	0.009	1.1	0.015	1.3	[30]
1136+1551	1.1879	0.34	1.6	0.78	1.4	[41, 65, 90–92]
1239+2453	1.3824	–	–	1.63	1.4	[41]
1744−1134	0.0041	0.004	1.1	0.006	1.3	[30]
1918−0449	2.479	1.47	1.2	2.31	1.1	[40]
1921+2153	1.3373	1.30	2.0	1.54	1.6	[41, 88]
1932+1059	0.2265	0.12	1.3	0.42	1.7	[38, 41, 90]
1946+1805	0.4406	0.24	2.0	0.75	1.1	[41, 65, 88]
2004+3137	2.1112	–	–	1.18	1.3	[41]
2018+2839	0.5579	0.17	1.2	0.76	1.2	[38, 41, 64, 65, 88]
2022+2854	0.3434	0.11	2.0	0.50	1.1	[41, 88]
2113+2754	1.2028	–	-	1.13	1.1	[41]
2144−3933	8.5098	5.90	1.1	11.8	1.1	[83]
2145−0750	0.0161	0.011	1.1	0.017	1.2	[29]
2251−3711	12.123	10.0	2.0	–	–	[84]
2317+2149	1.4447	–	–	1.01	1.1	[41]

Width, τ_μ, and quasi-periodicity, P_μ, of quasi-periodic sub-structures are determined for pulsars and sources not already listed in Table 2, as inferred from the literature. We quote the name of the source, the rotation period, P, and the geometric mean (GM) and the geometric standard deviation factor (GSTD) computed for values obtained from the references listed in the last column. Note that it is often more reliable to measure periodicities rather than widths, resulting in more measurements for the former. See text for details.